New Method for Determining Mineralogy and Matrix Properties From Elemental Chemistry Measured by Gamma Ray Spectroscopy Logging Tools

R. Freedman, S. Herron, V. Anand, M. Herron, D. May, and **D. Rose,** Schlumberger

Summary

Methods for predicting mineralogy from logging-tool measurements have been an active area of research for several decades. In spite of these efforts, methods for predicting quantitative mineralogy including clay types from well-logging data were not fully achieved. The introduction of geochemical logging tools in the 1980s offered promise; however, early versions of geochemical logging tools did not measure elemental chemistry with enough accuracy and precision to enable reliable and quantitative determination of mineralogy. Recent advances in geochemical-logging-tool technology now enable accurate and robust measurements of the chemical elemental concentrations that are needed to determine continuous quantitative and detailed logs of mineralogy.

This paper presents a novel approach for determining more accurate and more detailed mineralogy from an elemental spectroscopy logging tool. This work was made possible by three recent developments: the introduction of a new neutron-induced gamma ray spectroscopy logging tool, a new research database consisting of chemistry and mineralogy measured on cores acquired worldwide from conventional and unconventional reservoirs, and a new model-independent inversion method that overcomes the limitations of previous model-dependent methods.

The model-independent inversion makes use of the database that includes clean sands, shaly sands, shales, carbonates, and complex mixed lithologies. The database contains laboratory measurements of dry-weight elemental chemistry and mineralogy measured by transmission Fourier-transform infrared (FTIR) spectroscopy. The database is used to derive a model-independent mapping function that accurately represents the complex functional relationship between the elemental concentrations and the mineral concentrations. After the mapping function is determined from the database, one can use it to predict quantitative mineralogy from elemental concentrations derived from the logging-tool measurements. Unlike previous inversion methods, the model-independent mapping function does not have any adjustable parameters or require any user inputs such as mineral properties or endpoints.

The mapping function is used to predict continuous logs of matrix densities plus concentrations of 14 minerals (i.e., illite, smectite, kaolinite, chlorite, quartz, calcite, dolomite, ankerite, plagioclase, orthoclase, mica, pyrite, siderite, and anhydrite) from eight dry-weight elemental concentrations derived from the logging tool. The new method was applied to well-log data acquired worldwide in numerous conventional and unconventional reservoirs with a wide variety of complex mineralogies. The predicted mineralogies and matrix densities are generally found to be consistent with core-derived mineralogies and matrix densities.

This paper (SPE 170722) was accepted for presentation at the SPE Annual Technical Conference and Exhibition, Amsterdam, 27–29 October 2014, and revised for publication. Original manuscript received for review 6 November 2014. Revised manuscript received for review 4 June 2015. Paper peer approved 3 August 2015.

Introduction

The early attempts in the late 1970s and the 1980s at predicting mineralogy from well-logging data preceded geochemical logging and mostly relied on nuclear tool measurements such as spectral natural gamma ray (Th, U, K), neutron, density, sonic, and photoelectric absorption logs. The interpretation of these measurements provided agreeable results in some environments and could quantify major lithological units such as shales, sands, and carbonates. However, these measurements did not have sufficient sensitivity to allow for the determination of complex mineralogy. Modern neutron-induced gamma ray spectroscopy or geochemical logging tools evolved from the carbon/oxygen (C/O) tools that were introduced in the 1970s to provide salinity-independent estimates of oil saturations (Culver et al. 1974). An important paper by Hertzog (1980) discussed an experimental inelastic scattering-and-capture neutron-induced gamma ray logging tool for measuring C/O as well as Si, Ca, and Fe yields to be used for lithology delineation. This paper signaled the birth of modern geochemical logging. Since 1980, geochemical-logging-tool technology has passed through multiple phases of development with continuing improvements in technology including improved neutron sources, electronics, and scintillation detectors (Pemper et al. 2006; Galford et al. 2009; Radtke et al. 2012). These technological advances resulted in more measured elemental concentrations with improved precisions and accuracies, thus providing an opportunity for more quantitative and more detailed mineralogy analysis. This paper presents a model-independent inversion method developed to take full advantage of a new quality-controlled worldwide chemistry-and-mineralogy research-core database and the more-accurate and -robust elemental concentrations measured by a new geochemical logging tool (Radtke et al. 2012).

Importance of Mineralogy. Detailed and accurate knowledge of mineralogy is essential for understanding the complexity of conventional and unconventional reservoirs. It provides vital information needed for the evaluation, completion, and production of hydrocarbons. The following examples illustrate the importance of knowing detailed and quantitative mineralogy.

It is well-known that logging-tool measurements are strongly affected by the different lithologies and minerals present in the rocks. For example, clay minerals such as smectite have a large cation-exchange capacity, which provides an additional conductivity mechanism in clastic reservoir rocks. The clay conductance becomes a significant effect in the presence of low- salinity formation waters (Waxman and Smits 1968). The excess conductivity arising from the clays reduces the log-measured resistivities, which can result in underestimation of hydrocarbon saturations. Moreover, the equations and models used to derive key formation properties from tool responses require knowledge of rock-matrix properties, such as matrix densities, hydrogen indices, neutron-absorption cross sections, sonic-wave velocities, and dielectric constants, which can be more accurately determined when the mineralogy is known.

Detailed knowledge of mineralogy is also needed for optimizing completions to achieve maximum well production. Knowing

the concentrations of clays and other minerals present in a petroleum-bearing formation is vital for determining the completion and stimulation fluids that one should use to optimize production rates and to avoid near-wellbore formation damage. For example, it is well-known that acidizing formations that contain chlorite causes precipitation of iron, which plugs pore throats and greatly reduces the permeability in the vicinity of the wellbore. Similarly, during well completions, one should avoid the injection of low-salinity water into formations containing smectite because smectite absorbs water and swells to a larger volume, thereby reducing the permeability. Accurate knowledge of the clay types and their concentrations is needed to prevent the problem of fines migration. For example, if it is known that illite and kaolinite are present, one can lower the flow rates from the well to minimize the chances of dislodging fine particles and damaging the formation.

Shortcomings of Model-Dependent Inversion Methods. Previous methods for predicting mineralogy are based on models. Model-dependent inversion methods require user inputs such as mineral compositions and mineral endpoints as well as subjective assumptions about which minerals are present and should be included in the model. Computerized log-interpretation systems for predicting lithology and mineralogy (Mayer and Sibbit 1980; Quirein et al. 1986; Freedman and Puffer 1988) are based on simultaneous model-dependent inversions of suites of logging-tool measurements. Theoretical tool-response equations or forward models are used to represent the logging-tool measurements. The tool-response equations are functions of the reservoir properties including the lithologies and mineral concentrations to be determined. The predicted reservoir properties and mineral concentrations are determined by minimizing cost functions, which are weighted sums of the differences between the measured tool responses and the response equations. There are usually not enough independent measurements to solve for the many minerals that can be present. The model-based inversions attempt to circumvent this problem by requiring the user to select a "mineral model" that specifies a subset of minerals for which the minimization determines the concentrations. Clearly, assuming a mineral model is not a reliable method for predicting mineral concentrations when there are additional minerals present that are not in the assumed mineral model. Another shortcoming of model-based inversions is that the models require specification of mineral endpoints such as densities, hydrogen indices, dielectric constants, and thermal neutron-absorption cross sections. Accurate mineral compositions and properties are not known because mineral compositions and properties can vary. This variability is especially notable for the more-complex minerals such as the clays, micas, and feldspars. Requiring users to enter mineral properties, compositions, and mineral models is one of the shortcomings of model-based inversion methods. It means that mineralogy predictions from model-dependent methods are user-dependent because different log analysts can predict different lithologies and mineral concentrations from the same suite of well-logging measurements.

Linear-regression models were also used to predict mineralogy. This approach is based on empirically developed linear-regression equations for which the coefficients are found by fitting the equations to a core database of elemental chemistry and mineralogy (Herron and Herron 1996). This sequential approach uses different regression equations, depending on the feldspar concentration. Another recently published method uses the bulk elemental composition to first determine lithology and constrain the mineral selection, and then a sequential mass-balance approach to solve for selected minerals (Pemper et al. 2006; Jacobi et al. 2008).

Developments Now Enabling Quantitative and Detailed Mineralogy Prediction

This section discusses the confluence of three recent developments that enable quantitative and detailed mineralogy determination from elemental spectroscopy logging-tool measurements.

New High-Performance Spectroscopy Logging Tool. The recent development of a new high-performance neutron-induced gamma ray spectroscopy geochemical logging tool (Radtke et al. 2012) is one of three critical developments that finally enable the prediction of detailed and quantitative mineralogy from well logs. The advanced technology in the new geochemical tool includes a high-output pulsed-neutron generator (PNG), a high-resolution $LaBr_3$:Ce scintillation detector, and an advanced electronics-acquisition system to measure very high gamma ray count rates. The output of the PNG exceeds 3×10^8 neutrons per second, and the gamma ray count rate measured by the scintillation detector can exceed 2.5×10^6 counts per second. The high gamma ray count rate and the high resolution of the $LaBr_3$:Ce scintillation detector make possible the improved accuracy and precision of the derived dry-weight elemental concentrations.

The new tool measures gamma rays emitted by nuclei after thermal neutron capture and after inelastic scattering of fast neutrons. The processing of the detected gamma ray spectra provides accurate and precise dry-weight elemental concentrations including Si, Ca, Mg, Al, K, Fe, S, Mn, and C. The high precision and accuracy of these derived dry-weight elemental concentrations are essential for determining detailed and quantitative mineralogy and also total organic carbon.

Chemistry and Mineralogy Database. Another key development is the compilation of a quality-controlled database containing the elemental composition and mineralogy of more than 2,000 samples. The database includes core samples from clean sands, shaly sands, shales, carbonates, and mixed lithologies from both conventional and unconventional resources composed of varying geologic ages, depositional environments, and degrees of diagenesis from around the world. Thus, the mineral assemblages are representative of common hydrocarbon-bearing sedimentary environments. However, radial-basis mapping functions (RBFs) are only as useful as the data on which they are based, and some carbonate environments were not represented in available samples. Notably missing were pure anhydrites, dolomites, and some calcite mixtures common in carbonate environments such as the Middle East. These holes in the database were filled with artificially constructed mixtures of carbonates and evaporites to minimize nonlinearity effects from missing data.

Careful quality control was exercised for all samples, according to procedures described by Herron et al. (2014). Samples were crushed, homogenized, and split with a rotary splitter, and identical splits were used to measure chemical and mineral composition. Chemical concentrations were measured by a combination of X-ray fluorescence (XRF), inductively coupled plasma mass spectrometry (ICP/MS), and LECO by SGS. The accuracy of these measurements was vetted by blind analyses of Certified Reference Materials from National Institute of Standards and Technology (NIST), U.S. Geological Survey (USGS), and other similar organizations. The mineralogy was determined by transmission dual-range FTIR spectroscopy (Herron et al. 1997). The quality of all measurements was monitored with the QCMin procedure in which the mineral concentrations determined for each sample are multiplied by the chemical compositions of those minerals and summed to produce a mineral-based estimate of the multiple-element sample's chemical composition. The estimated chemical composition is then compared, element by element, with the measured chemical composition to provide a measure of the consistency between the two independent measurements. Because the elemental composition was certified, a close agreement between the measured and reconstructed composition is an indication of overall data quality.

All minerals routinely analyzed by the FTIR procedure are included in the database after grouping polymorphs (e.g., calcite and aragonite or quartz and chert). The final mineral assemblage includes 14 minerals: illite, smectite, kaolinite, chlorite, quartz, calcite, dolomite, ankerite, plagioclase, orthoclase, mica, pyrite, siderite, and anhydrite. Hydrous minerals such as gypsum and opal are rare, but where present, they are treated as their anhydrous

counterparts anhydrite and quartz, respectively. Barite concentrations higher than 2 wt% are extremely rare and treated as contamination and removed. Minor and trace minerals, such as magnetite, zircon, rutile, etc., are not detected by our FTIR techniques, but the compositional variability caused by their presence is captured in the elemental data. Samples with minerals that are not common but can be present at high concentrations, such as apatite and rhodochrosite, are also not included in the database. In the final database selected for this study, major framework minerals, including quartz, calcite, dolomite, and anhydrite, are well distributed in the range of 0 to 100 wt%. Total clay content ranges from 0 to 92 wt%; illite is the dominant clay, averaging more than half the total clay content. Total feldspar concentrations range from 0 to 53 wt%. Mica (predominantly muscovite), pyrite, and siderite have maximum values near 30 wt%, and ankerite has a maximum of 40 wt%.

Model-Independent Inversion Method. The model-independent inversion method discussed in this paper was first proposed by Freedman (2006; 2007) as a new approach for solving complex reservoir-characterization problems for which accurate forward models are not known. It was already successfully used to solve a number of challenging problems (e.g., Anand et al. 2011; Gao et al. 2011; Freedman et al. 2012, 2013). Our paper is the first application of the method to the mineralogy problem. The model-independent inversion method relies on having a comprehensive calibration database of measurements. The database is used to derive a model-independent mapping function that accurately represents the functional relationship between the dry-weight elemental concentrations and the dry-weight mineral concentrations for all the samples in the database. The mapping function is expressed as a weighted sum of normalized Gaussian RBFs. The weights and the widths of the Gaussian functions are determined from the database.

The model-independent inversion method has a strong and well-established mathematical foundation. Applied mathematicians proved that RBF mapping functions provide more-accurate interpolations for multidimensional functions of many variables (Powell 2001) than do other interpolation methods. One of the attractive features of RBF interpolation is that neither densely populated nor large databases are required. Mathematicians have established that one can obtain accurate results with sparsely populated databases with scattered data (i.e., unevenly distributed) (Buhmann 2003). After the mapping function is derived from the database, it is used to predict continuous logs of mineral concentrations and matrix densities from dry-weight elemental concentrations measured by the new gamma ray spectroscopy logging tool.

The model-independent approach has many attractive features, including the following:

- It is easy to implement.
- It is applicable to both linear and nonlinear problems.
- It works well with sparsely populated databases.
- Mineral compositions and endpoints are not needed.
- No mineral model is assumed.
- Number of outputs can exceed number of inputs.
- There are no free parameters or subjective user inputs.

Log examples discussed later in this paper show predicted logs of 14 mineral concentrations (i.e., illite, smectite, kaolinite, chlorite, quartz, calcite, dolomite, ankerite, plagioclase, orthoclase, mica, pyrite, siderite, and anhydrite) plus matrix densities. The mineralogy logs are predicted from eight elemental concentrations (i.e., Si, Al, Ca, Mg, K, Fe, S, and Mn) measured by the new geochemical logging tool (Radtke et al. 2012).

Derivation of the RBF Mapping Function. This section summarizes the derivation of the RBF mapping function. To save space, some of the details are omitted, such as we do not display the normalized Gaussian functions that one can find in Freedman (2006). The latter paper also provides additional intuitive insight as to how the method works. Our objective here is to construct a mapping function from the database that one can use to predict mineralogy and matrix densities from an n-dimensional vector $\vec{x}$ of dry-weight elemental concentrations (e.g., $n=8$) measured by the logging tool. The mapping function, $\vec{F}(\vec{x})$, is an m-dimensional vector with elements that are the dry-weight mineral concentrations and the matrix densities (e.g., $m=15$) predicted from the log-derived elemental concentrations. The number of RBF outputs exceeds the number of measurements. This does not violate any rules of algebra because the mapping-function outputs are not determined by solving a system of equations but by interpolation in the multidimensional mineral output space. On the contrary, model-dependent inversions with constraints require approximately as many measurements as there are outputs because, to determine the outputs, one must solve a set of algebraic equations that arise from fitting the measurements to the model equations. This is the reason that model-dependent methods require use of a mineral model because there are seldom enough measurements to solve for all the minerals that can be present.

Consider a database of N samples in which the database measurements include dry-weight elemental concentrations, dry-weight mineral concentrations, and matrix densities. The mapping function is constructed from the database as follows. One can express the mapping function as a weighted sum of N normalized Gaussian functions (ϕ) called the RBFs,

$$\vec{F}(\vec{x}) = \sum_{i=1}^{N} \vec{c}_i \phi(||\vec{x} - \vec{x}_i||). \quad \ldots\ldots\ldots\ldots\ldots\ldots \quad (1)$$

The summation in Eq. 1 is over the N samples in the database, where $\vec{x}_i$ is a vector with components that are the dry-weight elemental concentrations (or a subset of the measured elemental concentrations) for the ith database sample. The weighting coefficient $\vec{c}_i$ in Eq. 1 is an m-dimensional vector associated with the RBF centered at the ith database sample. One can determine the widths of the Gaussian RBFs from the Euclidean nearest-neighbor distances of $\vec{x}_i$ in the input-measurement space. The mapping-function predictions are not overly sensitive to the Gaussian function widths, as discussed by Freedman (2006), and good results were achieved by choosing the widths to be equal to, or of the order of, the nearest-neighbor distances.

The arguments of the Gaussian RBFs in Eq. 1 are proportional to the squared Euclidean norms in the n-dimensional input space; for example,

$$\|\vec{x} - \vec{x}_i\|^2 = \sum_{p=1}^{n} (x_p - x_{p,i})^2. \quad \ldots\ldots\ldots\ldots\ldots\ldots \quad (2)$$

If the database inputs and outputs are required to satisfy Eq. 1, then the weighting coefficients $\vec{c}_i$ in Eq. 1 for fixed Gaussian widths are determined from the matrix equation,

$$C = \Phi^{-1} \cdot Y, \quad \ldots\ldots\ldots\ldots\ldots\ldots\ldots\ldots \quad (3)$$

where the $N \times N$ matrix Φ is positive-definite. Its matrix elements are normalized Gaussian RBFs for which the arguments are the Euclidean norms of all pair-wise differences of the database elemental concentrations:

$$\Phi_{i,j} = \phi(||\vec{x}_i - \vec{x}_j||) \quad 1 \le i,j \le N. \quad \ldots\ldots\ldots\ldots \quad (4)$$

The $N \times m$ matrix C contains the weighting coefficients, and the $N \times m$ matrix Y contains the measured database mineral concentrations and matrix densities for the database samples.

A few comments about the mapping function in Eq. 1 will be instructive. It follows from Eqs. 1 and 3, that, if the mapping function in Eq. 1 is evaluated at any database $\vec{x}_i$, then the mapping-function output exactly reproduces, to within computer precision, the database mineral concentrations and matrix densities for that sample. Another useful and perhaps nonobvious property of the mapping function in Eq. 1 is that the sum of the RBF-predicted mineral weight percentages automatically sums to 100 because the database mineral concentrations sum to 100%.

The RBF matrix (Φ) in Eq. 4 is positive-definite for Gaussian RBFs so that the inverse matrix in Eq. 3 always formally exists

Mineral	Database Range (wt%)	RBF Average Absolute Deviation (wt%)
Illite	0–55	2.0
Smectite	0–34	0.9
Kaolinite	0–68	0.9
Chlorite	0–25	0.9
Quartz	0–99	1.3
Calcite	0–100	1.1
Dolomite	0–100	1.0
Ankerite	0–40	0.6
Orthoclase	0–27	0.8
Plagioclase	0–44	1.3
Mica	0–29	1.0
Pyrite	0–22	0.3
Siderite	0–32	0.3
Anhydrite	0–100	0.4
Matrix density (g/cm^3)	2.63–3.09	0.008

Table 1—Summary of database mineral concentrations and average absolute deviations for RBF predictions.

and is nonsingular; however, if the condition number (ratio of the largest to the smallest eigenvalue) of the Φ matrix is large, then the weighting coefficients can contain numerical noise arising from the matrix inverse in Eq. 3. This noise can propagate by means of Eq. 1 to the predicted mineralogy logs.

We observed this problem in a few of the many well-logging data sets that we processed. Some of the predicted mineralogy logs had a spurious high-frequency character that was not consistent with either the vertical resolution of the tool or thin laminations in the reservoir. Plots of the weighting coefficients for each of the minerals confirmed that some of the coefficients were noisy. The condition number of the Φ matrix for our database was approximately 36,000. One can suppress the noise with mathematical regularization to reduce the condition number and filter out the noise that arises from the small eigenvalues in the Φ matrix. This was discussed by Freedman (2006). It leads to the following modification of Eq. 3,

$$C = (\Phi + \alpha \cdot I)^{-1} \cdot Y, \quad \ldots\ldots\ldots\ldots\ldots\ldots\ldots\ldots \quad (5)$$

where α is a nonnegative "regularization parameter." The regularization parameter in Eq. 5 multiplies the $N \times N$ identity matrix (I). The default value is $\alpha = 0$; however, if the predicted mineralogy logs appear noisy, then a small positive value of α can significantly reduce the condition number of the Φ matrix and filter out any numerical noise in the weighting coefficients. The regularization reduces noise and improves the repeatability of the logs. It can, however, introduce some bias, and therefore, the tradeoff between accuracy and precision determines how much regularization one should use. We found that, for our database, a regularization parameter equal to 0.5 significantly reduces the noise on the mineralogy logs without adversely affecting the fidelity of the predicted mineral concentrations and matrix densities.

One should note that, if a nonzero regularization parameter is used, then the RBF-predicted mineral percentage concentrations no longer sum to 100% because the regularization tends to slightly suppress them. One can renormalize the predicted concentrations so that they sum to 100%. Likewise, if Eq. 5 is used to compute the weighting coefficients in Eq. 1, then the mapping function evaluated at database inputs $\vec{x}_i$ closely approximates, but no longer exactly reproduces, the measured database mineral concentrations and matrix densities.

Accuracies of Mapping-Function Predictions. One can use the database itself to assess the accuracies that one can expect from the mapping-function predictions. This is performed with the so-called "leave-one-out" (LOO) method. In the LOO method, a sample is removed from the database, and the mapping function for the reduced database with $(N - 1)$ samples is computed. The mapping function from the reduced database is used to predict the mineral concentrations and the matrix density for the sample that was removed with the database elemental concentrations for the removed sample. The sample that was removed is restored to the database, another sample is removed, and this process is repeated for all N database samples. The results of the LOO method are the RBF-predicted mineral concentrations and matrix densities for the N database samples. Then, one can compute the deviations of each of the RBF predictions from the database values. The LOO method is time-consuming because it requires computing N mapping functions. The LOO method needs to be performed only to assess the accuracy of the mapping-function predictions.

The results of the LOO method applied to the worldwide database are summarized in **Table 1** and shown in **Fig. 1.** These results were computed with a regularization parameter equal to 0.5. The LOO was also applied without regularization, and the results (not shown here) showed very slightly higher average absolute deviations and slightly lower average deviations, as expected. The plots in Fig. 1 show RBF-predicted mineral concentrations on the y-axis and the measured values on the x-axis. On each plot, we show three statistical quantities characterizing the deviations (i.e., RBF predictions minus the measured values). These quantities are the average absolute deviation (aad), average deviation (ad), and correlation coefficient (cc).

The crossplots in Fig. 1 show comparisons of predicted and measured values for all database samples. For most of the 14 predicted mineral concentrations, the average absolute deviations, a measure of their scatter, are less than 1.0 wt%. Also, for the matrix density, the average absolute deviation is less than 0.01 g/cm^3. The average deviations, which are a measure of bias, are generally very small. Finally, the correlation coefficients are very good for most of the predicted mineral concentrations. Fig. 1 shows that the smallest relative errors and best correlation coefficients across the entire dynamic range are observed for the framework minerals: quartz, calcite, dolomite, and anhydrite. As a general rule, these are the easiest minerals to predict from elemental concentrations because their compositions do not tend to deviate significantly from their stoichiometric values, and their compositions do not highly correlate with each other. In contrast, a higher degree of scatter exists for the feldspar, clay, and mica minerals: orthoclase, plagioclase, illite, smectite, kaolinite, chlorite, and mica (predominantly muscovite). There are at least four inherent factors that cause this. First, these minerals are all aluminosilicates for which there are natural variations in composition. Second, there is a high degree of similarity in the compositions of many of these minerals. Third, there is a natural correlation in the occurrence of some minerals such as illite and smectite. Finally, most of these minerals have a limited dynamic range, as one can see in both Fig. 1 and Table 1.

Log Examples in Cored Wells

Logging Speed and Depth of Investigation. Logging speeds for the new neutron-induced gamma ray spectroscopy tool are typically in the range of 500 to 1,000 ft/hour which provides measurements with agreeable precision. The logs discussed in this paper were acquired at logging speeds in this range.

The integrated radial depth of investigation (DOI) (e.g., radius at which 90% of the measurements are derived) depends on porosity, fluid types, saturations, and borehole size. Modeling has shown that the DOI is generally in the range of approximately 6 to 10 in. and is comparable to that of neutron-porosity logging tools.

Processing Summary. This section discusses RBF processing of three unconventional wells for which core-measured mineralogy and matrix densities are available for comparison. The three wells are from very different areas and have very different lithologies and mineralogies. The RBF mapping function in Eq. 1 was used to process the elemental chemistry logs from the new geochemical logging tool. No other data were used to obtain the results shown in this section. RBF processing is simple and very fast because only the summation in Eq. 1 is needed, and hundreds of feet of elemental chemistry data from the new geochemical tool can be processed in a few seconds to produce continuous logs of mineral concentrations and matrix densities. It is worth repeating

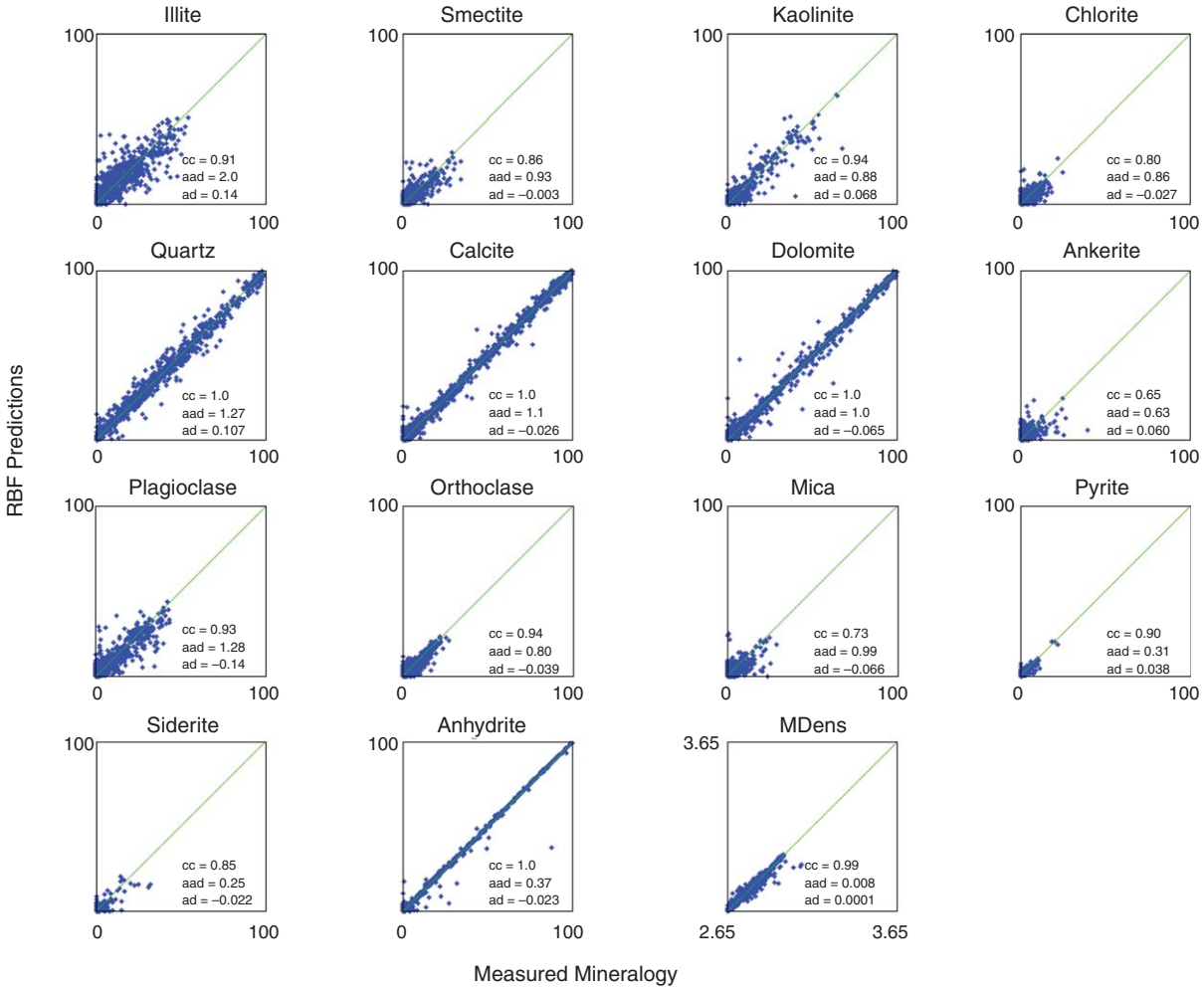

Fig. 1—RBF-predicted vs. measured dry-weight mineral concentrations in weight percentage and dry-weight matrix densities in g/cm^3 computed with the LOO method for a worldwide database including clean sands, shaly sands, shales, carbonates, and mixed lithologies. The average absolute deviations (aad) for all the predicted minerals except for illite are either close to or less than 1.0 wt%, and the aad for the predicted matrix densities (MDens) is less than 0.01 g/cm^3.

again that the RBF method does not require any user inputs or have any tunable parameters. All the log data shown in this section were processed with the same RBF mapping function. **Fig. 2** shows the eight elemental weight fractions that are the logging-tool inputs and the RBF mapping-function outputs, which are continuous logs of 14 mineral-weight fractions and the matrix density.

South Texas Eagle Ford Shale Well. The first log example is from a well drilled in the Eagle Ford shale formation in south Texas, which is one of the most prolific oil-producing reservoirs currently in North America. To the right of the depth track in **Fig. 3** are continuous logs of RBF-predicted mineral-weight fractions and matrix densities over the cored interval shown as solid curves. The solid circles are the core measurements. A color-coded

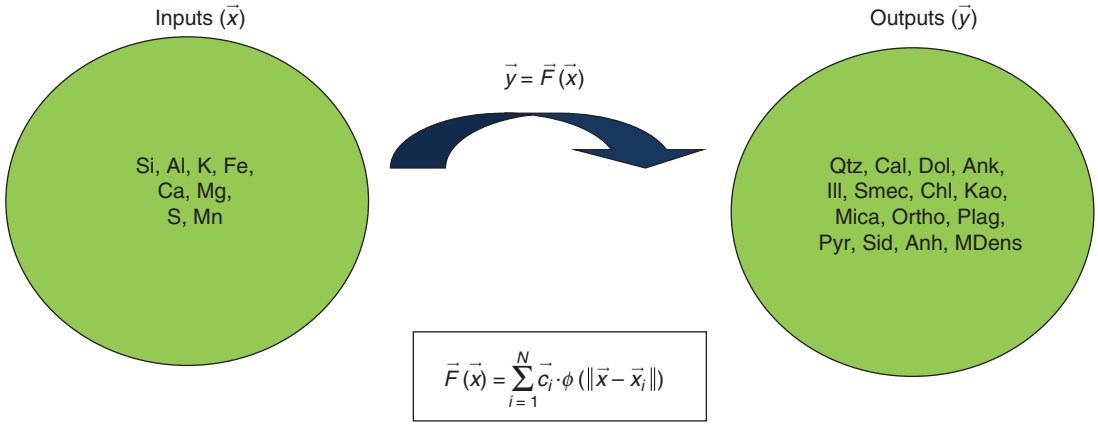

Fig. 2—A schematic of the RBF mapping-function processing of the geochemical logging-tool data. The elemental concentrations from the geochemical logging tool are inputs to the RBF mapping function (Eq. 1), which is shown here. The outputs of the mapping function are the 14 minerals and the MDens shown.

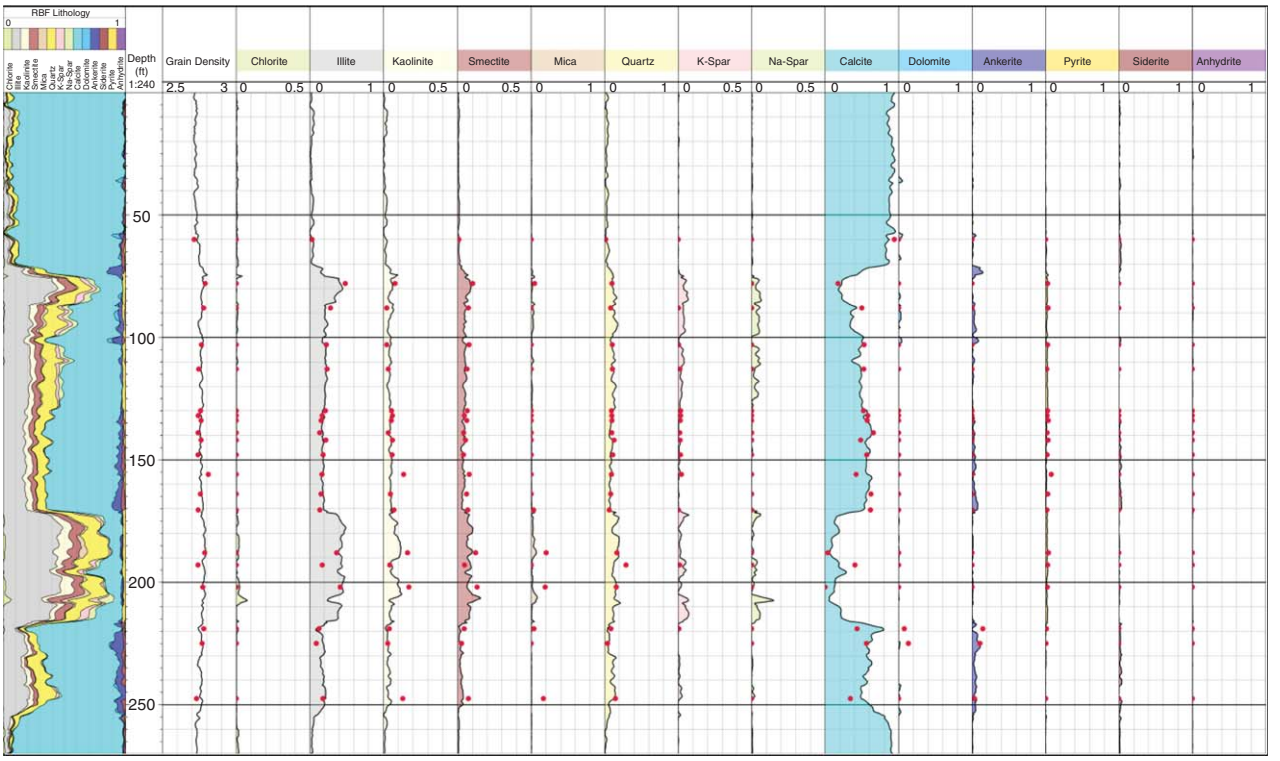

Fig. 3—RBF processing of the geochemical-tool data from an unconventional well in the Eagle Ford shale formation in south Texas. The curves in the tracks to the right of the depth track show continuous logs of RBF-predicted dry-weight matrix densities and mineral concentrations. The circles are the dry-weight matrix densities and mineral concentrations derived from core measurements. The core mineral concentrations were measured by FTIR. A color-coded lithology track is shown to the left of the depth track. Observe the good quantitative agreement between the log-predicted mineral concentrations and the core-measured concentrations in this complex formation.

lithology column is shown to the left of the depth track. The sum of the 14 RBF-predicted mineral fractions is equal to unity.

This well has a complex mixed lithology composed of significant amounts of calcite, quartz, and clay minerals. Although illite is, by far, the dominant clay mineral, there are measurable quantities of both kaolinite and smectite. Observe the excellent agreement between the RBF-predicted logs and the core measurements. In particular, note that the method correctly evaluates minerals that are quantitatively significant such as illite, kaolinite, smectite, quartz, and calcite. Equally important is the fact that the RBF does not predict or overestimate mineral fractions that are absent or present in only trace amounts, such as chlorite, muscovite, feldspars, and other carbonate minerals. It was not previously possible to quantitatively determine these complex minerals from well-logging data. The smectite concentration is particularly important because of its adverse impact on both conventional and unconventional resources, and here the predicted smectite concentrations are in good agreement with the measured values. The RBF-predicted dry-weight matrix densities shown in Fig. 3 are also in excellent agreement with dry-weight densities measured on the cores.

As a check on the integrity of the RBF-predicted logs in Fig. 3, we removed the 20 core samples in our database from this well. A reduced mapping function was computed from the remaining database samples. The reduced mapping function was used to reprocess the elemental chemistry. The mineralogy and matrix density results from the reduced database processing are essentially identical to the results in Fig. 3, which demonstrates the robustness of our worldwide database and the excellent generalization properties of RBF mapping functions. Similar tests performed with other wells also confirm this conclusion.

West Texas Wolfcamp Shale Well. The second log example is from a well drilled in the Wolfcamp shale in west Texas. To the right of the depth track in **Fig. 4** are continuous logs of RBF-predicted mineral-weight fractions and matrix densities over the cored interval shown as solid curves. The solid circles are the core measurements. A color-coded lithology column is shown to the left of the depth track. The sum of the 14 RBF-predicted mineral fractions is equal to unity.

The Wolfcamp shale is currently one of the most prolific unconventional oil reservoirs in the Permian Basin. There are three distinct cored intervals in this well with noncored intervals separating them, as one can see from the log in Fig. 4. The dominant minerals in this complex lithology are siliciclastics with only very small amounts of carbonate present. There are significant amounts of quartz and feldspars, for which the RBF-predicted mineral-weight fractions are in quantitative agreement with the core-weight fractions. Also present in this well are all four clay types, for which the RBF-predicted weight fractions are in good overall agreement with the core-measured values. The small amounts of ankerite predicted by the RBF processing are consistent with the small weight fraction measured on the cores. It is worth noting again that the RBF-predicted weight fractions do not overestimate the weight fractions for minerals such as pyrite, dolomite, and anhydrite, which are present only in trace amounts. The RBF dry-weight matrix densities are seen to be in quantitative agreement with the dry-weight matrix densities measured on cores.

Canadian Montney Shale Well. The third log example is from a well drilled in the Montney shale in Canada. To the right of the depth track in **Fig. 5** are continuous logs of RBF-predicted mineral-weight fractions and matrix densities over the cored interval shown as solid curves. The solid circles are the core measurements. A color-coded lithology column is shown to the left of the depth track. The sum of the 14 RBF-predicted mineral fractions is equal to unity.

This well has a complex mixed lithology with significant amounts of quartz, calcite, dolomite, plagioclase (Na feldspar), orthoclase (K feldspar), illite, and smectite, as shown in Fig. 5. There is good quantitative overall agreement between the RBF and core mineralogy. Particularly noteworthy is the quantitative prediction of quartz, clay minerals, and mica, which is very

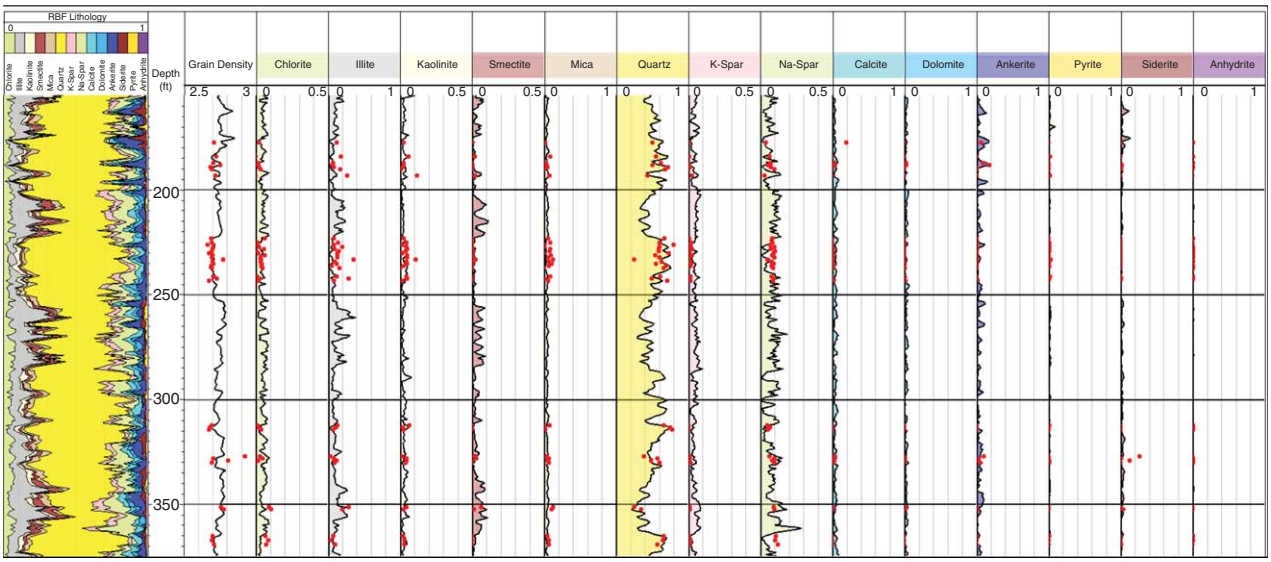

Fig. 4—RBF processing of the geochemical-tool data from an unconventional well in the Wolfcamp shale formation in west Texas. The curves in the tracks to the right of the depth track show continuous logs of RBF-predicted dry-weight matrix densities and mineral concentrations. The circles are the dry-weight matrix densities and mineral concentrations derived from core measurements. The core mineral concentrations were measured by FTIR. A color-coded lithology track is shown to the left of the depth track. Observe the good quantitative agreement between the log-predicted mineral concentrations and the core-measured concentrations in this complex formation.

challenging in the presence of so much feldspar, although the RBF-predicted feldspar is underestimated relative to that from core. Particularly noteworthy once again is the prediction of smectite concentrations that are consistent with the core measurements. The calcite and dolomite predictions are also reasonably good. The RBF-predicted matrix densities are observed to be in good agreement with the measured values.

Repeatability of Log-Derived Mineralogy. As discussed previously, the precision of the RBF-predicted mineral concentrations and matrix density logs is improved by using a nonzero regularization parameter (α) to compute the weighting coefficients in Eq. 1. Applying nonzero regularization reduces the condition number of the matrix inversion in Eq. 3 and serves to filter out numerical noise that arises from inverting the matrix. For all the results shown in this paper, we used a mapping function computed with a regularization parameter of 0.5 in Eq. 3. This reduces the condition number of the matrix inversion in Eq. 3 from 36,000 for $\alpha = 0$ to 4 for $\alpha = 0.5$. The regularization filters out the effects of the small eigenvalues in the Φ matrix. This causes no loss of information because the small eigenvalues contribute negligible information to the weighting coefficients.

Fig. 6 shows to the left of the depth track the RBF-predicted mineral concentrations for both a main and a repeat pass over an interval in a heavy-oil well in the San Joaquin Valley, California. To the right of the depth track are logs of elemental concentrations. The mineral concentrations and matrix densities predicted for the two passes are in good overall agreement. The larger

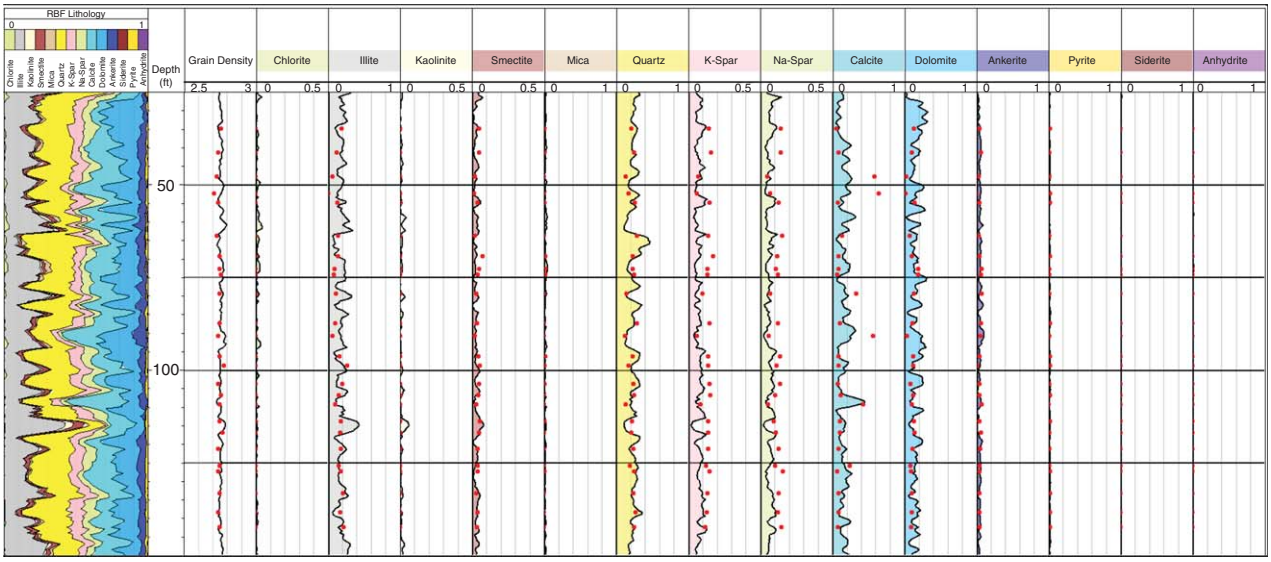

Fig. 5—RBF processing of the geochemical-tool data from an unconventional well in the Montney shale formation in Canada. The curves in the tracks to the right of the depth track show continuous logs of RBF-predicted dry-weight matrix densities and mineral concentrations. The circles are the dry-weight matrix densities and mineral concentrations derived from the core measurements. The core mineral concentrations were measured by FTIR. A color-coded lithology track is shown to the left of the depth track. There is good overall agreement between the predicted and the core-measured mineral concentrations in this very complex formation.

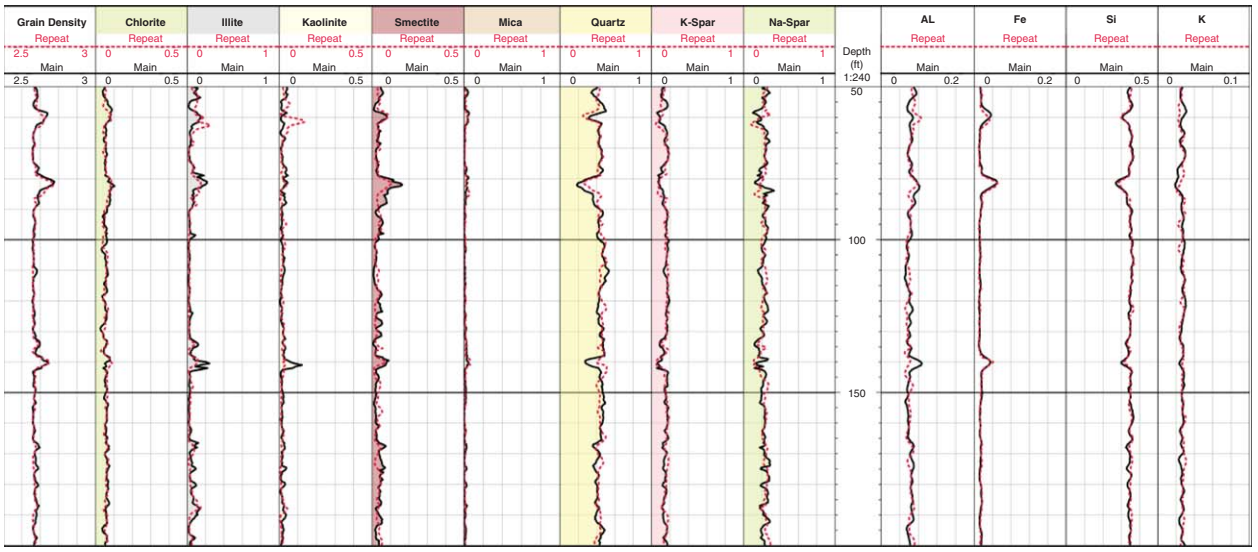

Fig. 6—Continuous logs of RBF-derived matrix densities and mineral concentrations for both a main and a repeat pass in a well drilled in the San Joaquin Valley, California. The RBF-predicted logs for the two passes are shown in the tracks to the left of the depth track. The tracks to the right of the depth track show the elemental concentrations of a few important elements from the two passes. The RBF-predicted matrix densities and mineral concentrations for the two passes agree well except in a few intervals in which the elemental concentrations for Al and K do not repeat very well.

differences between the main and repeat mineralogy logs at some depths are caused by differences in the main and repeat log elemental concentrations, especially in the Al and K weight fractions. It should be clear from this example that quantitative log predictions of mineral fractions and matrix densities are possible only when one can measure accurately the elemental concentrations with high precision. This requires a high-performance geochemical tool with accurate data-processing algorithms, including borehole corrections that can generate accurate and precise elemental concentrations.

Quality Checks on RBF Mineralogy Predictions. This section addresses the important question of how one detects when the input elemental chemistry data are not well-represented by the calibration database samples and therefore when one should flag the RBF predictions as not trustworthy. The question of what to do when we are "outside of the database" is not specific to the RBF method but is relevant to all empirically derived methods that are based on databases. For example, Archie used a core database of clean Gulf Coast sandstone formations to derive his famous saturation equation. It is well-known that the equation does not account for clay-conductance effects in freshwater shaly sand formations, where it underestimates oil saturations.

Two of the RBF quality-control checks are based on a level-by-level analysis of the elemental-concentrations vector that is input from the logging tool. The first quality check is to test whether each of the eight input elemental concentrations (e.g., Si, Al, Ca, Mg, K, Fe, S, and Mn) is within the range of the database chemistry. If a single input elemental concentration is outside the database range for that element, then a warning flag is turned on at the depths for which this occurs.

The second quality check can detect a situation in which the input elemental chemistry falls within the database range but might be near the edge or boundary of the database. In this case, there might be too few nearby database samples for accurate RBF interpolation. To address this case, we compute the Euclidean distances of the input elemental-concentrations vector from the database elemental concentrations. A "proximity flag" is turned on if there are less than a specified number of database samples (e.g., four) within a specified Euclidean radius in the elemental-chemistry space. This radius is on the order of the average of the database nearest-neighbor distances used to determine the widths of the Gaussian RBFs. One can determine the optimal number of nearby database neighbors and the optimal radius by simulation and confirm with field data.

The third quality check uses the RBF-predicted dry-weight mineral concentrations to compute reconstructed or theoretical dry-weight elemental concentrations. The elemental-reconstruction computation assigns fixed elemental compositions to each mineral. The theoretical elemental-concentrations computation is conducted for the major elements present in sedimentary rocks (i.e., Si, Al, K, Fe, S, Ca, Mg, and Na). One can detect incorrectly predicted mineral concentrations in intervals in which there are significant deviations between the reconstructed elemental concentrations and the log-derived elemental concentrations. The usage and interpretation of reconstructed elemental concentrations to quality check mineralogy are discussed in much more detail by Herron et al. (2014). One can use deviations between the reconstructed and tool-derived elemental concentrations to flag intervals in which the predicted mineral concentrations are likely to be incorrect.

Although our existing database contains samples of clean sands, shaly sands, shales, carbonates, and mixed lithologies, one could expand it in future developments and make it more comprehensive by adding additional core data for which the mineralogy is absent or not well-represented by the existing database. Of course, any added core chemistry and mineralogy data must be of the same high quality as the data in the existing database to enable quantitative mineralogy predictions. After the database is augmented with the new data, it takes only a few minutes of computer time to compute a new and more-universal RBF mapping function.

Conclusions and Summary

This paper presents a robust, general-interpretation procedure to quantitatively derive accurate, detailed mineral concentrations from geochemical-tool-logging data. This work helps to solve a long-standing and important problem in formation evaluation. It was made possible by the confluence of the three recent developments of a new geochemical logging tool, a new quality-controlled worldwide core database of measured dry-weight elemental concentrations and dry-weight mineral concentrations, and a new model-independent inversion method. All three of these recent developments are equally important and are essential enablers for quantitative mineral predictions.

We discussed the high-output neutron generator, high-resolution scintillation detector, and advanced electronics in the new geochemical logging tool. These advances in technology together with improvements in data processing make it possible to derive, from the measured gamma ray spectra, robust and accurate

elemental concentrations including Si, Al, Ca, Mg, K, Fe, S, and Mn. These elements are absolutely essential for quantitative and detailed mineralogy prediction in sedimentary rocks.

The database includes cores from conventional and unconventional reservoirs worldwide. The measurements on the database cores include dry-weight elemental concentrations, dry-weight mineral concentrations measured by FTIR spectroscopy, and dry-weight matrix densities. We also discussed database quality checks that were used to ensure the consistency of the measured elemental concentrations and the measured mineral concentrations. The quality checks are essential to ensure the construction of an accurate calibration database, which is essential for developing and testing methods for quantitative and detailed mineralogy predictions. Continuing investment in the database expansion to include minerals that are not represented in the current database might ultimately achieve a more-universal database that can predict accurate mineralogy anywhere in the world as well as improve the accuracy of the RBF-predicted mineralogies.

The new model-independent inversion method uses an RBF mapping function derived from the calibration database to predict quantitative and detailed mineral concentrations and matrix densities. The shortcomings of traditional model-dependent inversion methods are discussed. The features of the new model-independent method that overcome the limitations of the model-dependent methods are discussed. The derivation of the RBF mapping function from the database is explained. The LOO method by which one can determine the expected accuracies of the RBF mapping function from the database is explained, and results of the LOO method are shown and discussed.

We processed a subset of the elemental-concentrations data acquired by the new geochemical logging tool in three unconventional shale wells. The same RBF mapping function was used to process the data from all three wells. The inputs to the RBF mapping function were continuous logs of the eight dry-weight elemental concentrations (i.e., Si, Al, Ca, Mg, K, Fe, S, and Mn) derived from the logging-tool measurements. The outputs from the RBF mapping function were continuous logs of 14 dry-weight mineral concentrations (i.e., illite, smectite, kaolinite, chlorite, quartz, calcite, dolomite, ankerite, orthoclase, plagioclase, mica, pyrite, siderite, and anhydrite) plus the matrix density. The RBF-predicted minerals and matrix densities were compared with core results. The core mineralogy was measured with FTIR spectroscopy. The comparisons of the RBF-predicted and core-measured dry-weight mineral concentrations and matrix densities are shown to be in good overall agreement. These predictions were obtained without using any adjustable parameters or user inputs.

We discussed three quality checks on the RBF-predicted mineralogy. The input elemental concentrations are tested at each depth to determine if they are within the range of the database concentrations. Another test determines the proximity of the input elemental concentrations at each depth to the database samples to determine if there are enough nearby samples to provide accurate RBF interpolation. If these tests show that the input data are "outside the database" at some depth, then a warning flag is used to indicate that the predicted mineralogy and matrix density are questionable at that depth. The third quality check compares elemental concentrations from the logging tool at each depth with those reconstructed from the predicted mineralogy. Significant deviations between the elemental concentrations from the logging tool and the reconstructed concentrations are indicative of errors in the predicted mineralogy.

Nomenclature

$\vec{c}_i$ = m-dimensional vector of weighting coefficients for the ith database sample for $i = 1, \ldots, N$
C = $N \times m$ weighting matrix with rows that are the vectors, $\vec{c}_i$
$\vec{F}(\vec{x})$ = m-dimensional RBF mapping function defined in Eq. 1
m = dimensionality of the RBF mapping function (i.e., equal to the number of mineral-concentration outputs plus one)
n = number of independent variables in the mapping function (i.e., equal to the number of elemental-concentration inputs)
N = number of samples in the database
$\vec{x}$ = n-dimensional vector with elements that are the elemental-concentrations input from the logging tool
$\vec{x}_i$ = n-dimensional vector with elements that are the elemental concentrations for the ith database sample
Y = $N \times m$ matrix with elements that are the mineral concentrations and matrix densities of the database samples
α = nonnegative regularization parameter in Eq. 3
$\phi(||\bullet||)$ = normalized Gaussian RBF
Φ = $N \times N$ RBF matrix with elements, $\Phi_{i,j} = \phi(||\vec{x}_i - \vec{x}_j||)$
$||\bullet||$ = double bars denoting the Euclidean norm of the vector argument

Acknowledgments

It is a pleasure to thank Jim Grau and Jack Horkowitz for developing the algorithms used to derive the elemental concentrations from the measured gamma ray spectra. Also, thanks to the LithoScanner project team for their support and to the SDR Petrolabs staff for core analyses. We also owe thanks to Aria Abubakar, Farid Hamichi, Ridvan Akkurt, Daniel Codazzi, and Vlad Tertychnyi for managerial support and to Schlumberger for permission to publish this paper.

References

Anand, V., Freedman, R., Crary, S. et al. 2011. Predicting Effective Permeability to Oil in Sandstones and Carbonates From Well-Logging Data. *SPE Res Eval & Eng* **14** (6): 750–762. SPE-134011-PA. http://dx.doi.org/10.2118/134011-PA.

Buhmann, Martin D. 2003. *Radial Basis Functions: Theory and Implementations*, first edition, Cambridge University Press.

Culver, R. B., Hopkinson, E. C., and Youmans, A. H. 1974. Carbon/Oxygen (C/O) Logging Instrumentation. *SPE J.* **14** (5): 463–470. SPE-4640-PA. http://dx.doi.org/10.2118/4640-PA.

Freedman, R. and Puffer, J. E. 1988. Self-Consistent Log Interpretation Method (SLIM): Application to Shaly Sands. *Proc.,* 29th SPWLA Annual Logging Symposium, San Antonio, Texas, USA, 5–8 June. SPWLA-1988-T.

Freedman, R. 2006. New Approach for Solving Inverse Problems Encountered in Well-Logging and Geophysical Applications. *Petrophysics* **47** (2): 93–111. SPWLA-2006-v47n2a1.

Freedman, R. 2007. Method for Determining Characteristics of Earth Formations. US Patent No. 7,309,983.

Freedman, R., Anand, V., Zhou, T. et al. 2012. A Modern Method for Using Databases to Obtain Accurate Solutions to Complex Reservoir-Characterization Problems. *SPE Res Eval & Eng* **15** (4): 453–461. SPE-147169-PA. http://dx.doi.org/10.2118/147169-PA.

Freedman, R., Anand, V., Catina, D. et al. 2013. Major Advancement in Reservoir-Fluid Analysis Achieved Using a New High-Performance Nuclear Magnetic Resonance Laboratory System. *Petrophysics* **54** (5): 439–456. SPWLA-2013-v54n5-A3.

Galford, J., Truax, J., Hrametz, A. et al. 2009. A New Neutron-Induced Gamma ray Spectroscopy Tool for Geochemical Logging. *Proc.,* 50th SPWLA Annual Logging Symposium, The Woodlands, Texas, USA, 21–24 June. SPWLA-2009-40058.

Gao, B., Wu, J., Chen, S. et al. 2011. New Method for Predicting Capillary Pressure Curves From NMR Data in Carbonate Rocks. *Proc.,* 52nd SPWLA Annual Logging Symposium, Colorado Springs, Colorado, USA, 14–18 May. SPWLA-2011-HH.

Herron, S. L. and Herron, M. M. 1996. Quantitative Lithology: An Application for Open and Cased-Hole Spectroscopy. *Proc.,* 37th SPWLA Annual Logging Symposium, New Orleans, USA, 16–19 June. SPWLA-1996-E.

Herron, M. M., Matteson, A., and Gustavson, G. 1997. Dual-Range DR-FTIR Mineralogy and the Analysis of Sedimentary Formations.

Presented at the Society of Core Analysts Conference, Calgary, 7–10 September. SCA-9729.

Herron, S., Herron, M., Pirie, I. et al. 2014. Application and Quality Control of Core Data for the Development and Validation of Elemental Spectroscopy Log Interpretation. *Petrophysics* **55** (5): 392–414. SPWLA-2014-v55n5a2.

Hertzog, R. C. 1980. Laboratory and Field Evaluation of an Inelastic Neutron Scattering and Capture Gamma Ray Spectrometry Tool. *SPE J.* **20** (5): 327–340. SPE-7430-PA. http://dx.doi.org/10.2118/7430-PA.

Jacobi, D., Gladkikh, M., LeCompte, B. et al. 2008. Integrated Petrophysical Evaluation of Shale Gas Reservoirs. Presented at the CIPC/SPE Gas Technology Symposium Joint Conference, Calgary, 16–19 June. SPE-114925-MS. http://dx.doi.org/10.2118/114925-MS.

Mayer, C. and Sibbit, A. 1980. Global, A New Approach to Computer-Processed Log Interpretation. Presented at the SPE Annual Fall Technical Conference and Exhibition, Dallas, USA, 21–24 September. SPE-9341-MS. http://dx.doi.org/10.2118/9341-MS.

Pemper, R., Sommer, A., Guo, P. et al. 2006. A New Pulsed Neutron Sonde for Derivation of Formation Lithology and Mineralogy. Presented at the SPE Annual Technical Conference and Exhibition, San Antonio, Texas, USA, 24–27 September. SPE-102770-MS. http://dx.doi.org/10.2118/102770-MS.

Powell, M. J. D. 2001. Radial Basis Function Methods for Interpolation to Functions of Many Variables. *Proc.,* Fifth Hellenic-European Conference on Computer Mathematics and Its Applications, Athens, Hellas, 20–22, 2–24 September.

Quirein, J., Kimminau, S., LaVigne, J. et al. 1986. A Coherent Framework for Developing and Applying Multiple Formation Evaluation Models. *Proc.,* 27th SPWLA Annual Logging Symposium, Houston, USA, 9–13 June. SPWLA-1986-DD.

Radtke, R. J., Lorente, M., Adolph, B. et al. 2012. A New Capture and Inelastic Spectroscopy Tool Takes Geochemical Logging to the Next Level. *Proc.,* 53rd SPWLA Annual Logging Symposium, Cartagena, Colombia, 16–20 June. SPWLA-2012-AAA.

Waxman, M. H. and Smits, L. J. M. 1968. Electrical Conductivities in Oil-Bearing Shaly Sands. *SPE J* **8** (2): 107–122. SPE-1863-A. http://dx.doi.org/10.2118/1863-A.

Robert (Bob) Freedman is a scientific adviser at Schlumberger's Houston Formation Evaluation Center. His current research and engineering interests include nuclear magnetic resonance (NMR), electromagnetic (EM), and nuclear logging; downhole-fluid analysis; well-log analysis methods for shale reservoirs; and inversion of measurements in complex systems. Freedman holds more than 35 US patents on formation-evaluation technology and has authored or coauthored more than 60 formation-evaluation papers on a wide range of topics. He holds a PhD degree in theoretical condensed-matter physics from the University of California. Freedman has served as an SPE Distinguished Lecturer and an SPE Distinguished Author, and was awarded the SPE Cedric Ferguson Award. He served on the SPE Engineering Professionalism Committee.

Susan Herron retired in 2015 from her scientific adviser position in the Sensor Physics Department at the Schlumberger-Doll Research Center. During her 31 years with Schlumberger, she developed applications of elemental spectroscopy logs for source rock evaluation, elemental concentrations, formation-matrix properties, and mineralogy. Herron served as a Program Manager of Nuclear Sciences in SDR for 10 years. She holds geology degrees from Tufts University and State University of New York at Buffalo. Herron is a member of SPE and Society of Petrophysicists and Well Log Analysts (SPWLA) and is a 2015 SPWLA Distinguished Lecturer.

Vivek Anand is the Manager of Interpretation Engineering for NMR Answer Products at Schlumberger. He is also leading the development of Schlumberger's latest generation NMR-logging technology. Anand earned a BS degree from Indian Institute of Technology, New Delhi, and a PhD degree from Rice University, both in chemical engineering. He has authored or coauthored more than 20 technical papers and holds 10 US patents and patent applications. Anand is an associate editor for *Petrophysics* and *Interpretation* journals. He was an SPWLA distinguished speaker in 2009, the recipient of best-paper awards for the 2005 and 2013 SPWLA Annual Symposium, and recipient of the2011 SPE Young Professional best-paper award.

Michael Herron is a scientific adviser at Schlumberger-Doll Research. His research interests include inorganic geochemistry, mineralogy, and petrophysics. Herron has authored or coauthored more than 100 technical papers and holds 16 patents. He holds a PhD degree in geological sciences from State University of New York, Buffalo. Herron is a member of SPE.

Dale H. May is a retired petrophysicist. His 34-year history with Schlumberger included being a field engineer and an interpretation development petrophysicist. May holds a BS degree in physics from Texas Tech University.

David Rose is a principal petrophysicist with Schlumberger, based in Sugar Land, Texas, USA. His current interests include development and interpretation of nuclear-logging tools. Rose has a BS degree in geophysical engineering from Colorado School of Mines.